Journal of Mechanical Engineering Research and Developments
ISSN: 1024-1752
CODEN: JERDFO
Vol. 43, No. 6, pp. 472-486
Published Year 2020

Combined free and forced convection inside an enclosure

Mustafa Abdul Salam Mustafa†, Lina Jassim‡, Nazar Yasir Jasim‡†, Laith Jaafer Habeeb‡‡

†Air-Conditioning and Refrigeration Dep., Al Rafidain University Collage, Bagdad, Iraq,
‡Mechanical Engineering Department, Mustansiriyah University, Baghdad, Iraq
‡†Biomedical Engineering Department University of Technology, Baghdad, Iraq,
‡‡Training and Workshops Center, University of Technology, Bagdad, Iraq,

*Corresponding Author Email: Mustafa.altalib77@gmail.com; dr.linajassim@uomustansiriyah.edu.iq; nazarengineer777@gmail.com; laithhabeeb1974@gmail.com

ABSTRACT: This paper presents a numerical simulation to study the enclosed with force and free heat convection. Galerkin finite element approach was used for the numerical analysis, the investigated enclosure are square geometry with an inlet at the bottom and an opposite outlet at the top. Heat was applied to one side of the enclosure while the other walls were considered as an insulated wall. Reynolds number was changed during the tested from 25 to 300 (25, 50, 100, 150, 200, 250, 300), Richardson number was changed during the tested from 0 to 5 (0, 0.5, 1, 2.5, 5). The Nusselt number was calculated along the heated wall and as an average value, it was found that as the Reynolds and Richardson numbers increases, the Nusselt number is also increased. The isothermal lines and the streamlines were illustrated for different Reynolds and Richardson numbers.

KEYWORDS: Enclosure, Force convection, Finite elements, Nusselt number, Reynolds number, Richardson number.

INTRODUCTION

Enclosures and Cavities are common in several equipment and industries such as renewable energies, nuclear power, heat exchangers, etc. rectangular enclosures with natural convections was one of the first cases that was investigated using different end heated walls [1]. rectangular enclosures with natural convections is a field of several investigations due to its varied range engineering applications, which include the design of nuclear reactor, collectors of solar energy, electronic instruments cooling devices, building insulation, etc. the process has been studied and researched both experimentally and numerically in the past fifty years [2, 3]. Al-Balushi et al. numerically investigated the unsteady flow of free convection heat transfer through a square enclosure using nonhomogeneous dynamic model and Nano working fluids [4]. The vertical walls at both sides of the enclosure were thermally insulated whereas the wall at the base of the enclosure was maintained at uniform temperature and the wall at the top of the cavity was considered a cold wall.

The investigations showed that the average Nusselt number increases as the nanoparticles volume fraction and the thermal Rayleigh number intensify. Mehryan et al. numerically modeled the flexible partition displacement in a trapezoidal enclosure using the approach of The Fluid-Structure Interaction [5]. The result of the study illustrated that the enclosure heat transfer enlarged by increasing Rayleigh number. The cavity angle of inclination induces a small influence on the tensions induced but its effect on the heat transfer. Venkatadri et al. conducted a theoretical and numerical study of natural convection in two-dimensional laminar incompressible flow in a trapezoidal enclosure in the presence of thermal radiation [6]. The trapezoidal cavity has an inclined top wall, which in addition to the bottom wall is maintained at constant temperature, whereas the remaining (vertical side) walls are adiabatic. The computations indicate that local Nusselt number and velocity are increasing functions of the Rayleigh number and radiation parameter. Significant changes in streamlines, temperature contours and energy streamlines for high Rayleigh number are observed.

The energy flux vectors show that a large eddy is formed within the enclosure, which migrates towards the cold wall. Greater thermal buoyancy force accelerates the primary flow whereas it decelerates the secondary flow. Groulx et al. numerically studied a rectangular enclosure containing phase change material (PCM) melting [7]. The simulations was performed on a two dimensional model. The study showed that the maximum improvement on the thermal management of the PV-PCM panel is found when the PCM enclosure is prepared

with a full-width fin concurrently attached to the back and front plates. Bourdillon et al. implemented an investigation to study the phenomena of water freezing in internal geometries using solidification solvers [8]. Cavity of square shape was used along with inside a cylindrical enclosure. The results of the used model was compared with results found from the numerical models of CFD codes. Ezzaraa et al. numerically studied the interaction between laminar mixed convection and thermal radiation in a multiple vented rectangular enclosure, constant heat flux was used to keep it uniformly heated [9].

The study showed that the higher thermal performance was achieved by increasing the external flow velocity, the walls emissivity and when the enclosure outlet was placed on the cavity top wall at the middle. Motlagh et al. considered the free convection simulation of inclined porous semi-annulus enclosure filled with two-phase Nano fluid [10]. They found that Nusselt number is not the function of the enclosure inclination angle and the porosity number at low porous Rayleigh numbers. Additionally, Nusselt number rises by adding the nanoparticles volume fraction. Lee et al. discussed the influence of placing 3D obstacle in the middle of a horizontal cavity [11]. Geometry, which was taken into account, was horizontal enclosure with unit aspect ratio. The enclosure was cooled down from the top wall and heated from the base wall. At a small Rayleigh number, steady invariant solution was illustrated by the enclosure thermal behavior. Moreover, the thermal flow field was found by Picturing the 3D vertical structure. Park et al. numerically modeled a square enclosure as a two dimensional geometry with vertical arrangement of a hot circular and elliptical cylinders [12].

They found that the flow stability and thermal performance were affected by the inclination angle and position of the vertical cylinders. Qi et al. investigated heat transfer of Nano fluids (Fe3O4-water) natural convection in a rectangular enclosure with an adaptable magnetic field [13]. They reach the result that the Nusselt number start by increasing and afterward decreasing by increasing the mass fraction of nanoparticle. Additionally, they found that the vertical magnetic field improves the thermal performance. Zhang et al. numerically studied the steady-state natural convection in a cold outer square enclosure containing a hot inner elliptic cylinder [14]. They study results illustrated that the enclosure temperature contours and the streamlines were highly influenced by the outer square enclosure inclination angle, the inner cylinder size, and the Rayleigh number, meanwhile the enclosure inclination angle has a low influence on the average Nusselt number. In this paper, an enclosure with an opposite inlet and outlet was studied numerically. The convection used was both natural and forced convection. Finite elements was used for the investigation, Nusselt number, the isothermal lines, and streamlines was studied.

NUMERICAL METHOD

The schematic diagram of the problem shown in figure (1) illustrations that the enclosure analyzed in this paper consist of a square cavity with an inlet opening and outlet, the wall on the far side of the opening is heated externally while the other walls are set as insulated walls. Galerkin finite element approach was used for numerical analysis, the non-dimensional governing equations being solved by the model are:

The continuity equation

$$\frac{\partial u}{\partial y}+\frac{\partial \upsilon}{\partial y}=0 \tag{1}$$

X-Momentum equation

$$u\frac{\partial u}{\partial x}+\upsilon\frac{\partial u}{\partial y}=-\frac{\partial p}{\partial x}+\frac{1}{\mathrm{Re}}\left(\frac{\partial^2 u}{\partial x^2}+\frac{\partial^2 u}{\partial y^2}\right) \tag{2}$$

Y-Momentum equation

$$u\frac{\partial u}{\partial x}+\upsilon\frac{\partial u}{\partial y}=-\frac{\partial p}{\partial y}+\frac{1}{\mathrm{Re}}\left(\frac{\partial^2 \upsilon}{\partial x^2}+\frac{\partial^2 \upsilon}{\partial y^2}\right)+\left(\frac{Gr}{\mathrm{Re}^2}\right)T \tag{3}$$

Energy equation

$$u\frac{\partial T}{\partial x}+\upsilon\frac{\partial T}{\partial y}=\frac{1}{\mathrm{Re}.\mathrm{Pr}}\left(\frac{\partial^2 T}{\partial x^2}+\frac{\partial^2 T}{\partial y^2}\right) \tag{4}$$

Where, (u), (υ) are the dimensionless horizontal and vertical velocity components along (X) and (Y) directions, and (T), (p) are the dimensionless temperature and pressure.

The main governing parameters are:

Reynolds number (Re), Richardson number (Ri), and Prandtl number (Pr), they defined as

$$\mathrm{Re}=\frac{\upsilon_{in}L}{\nu} \tag{5}$$

$$Ri=\frac{Gr}{\mathrm{Re}^2} \tag{6}$$

$$Gr=\frac{g.\beta.L^3(T_h-T_{in})}{\nu^2} \tag{7}$$

$$\mathrm{Pr}=\frac{\nu}{\alpha} \tag{8}$$

Where, (α), (ν), and (ρ) are the thermal diffusivity, kinematic viscosity and density of fluid, and (g), (β) are the gravitational acceleration and the volumetric expansion coefficient.

In this study the Prandtl number (Pr) for air set as 0.71, the ratio between the opening to the length of the enclosure S/L = 0.2.

The computational domain in this method is normally subdivided roughly into a series of 448 separate macro-elements, as manifested in Figure (2). Then, the interior nodes to each macro-element can be generated within the run and spread in accordance to the Gauss-Legendre-Lobatto quadrature. So, the simulation accuracy can be enhanced via increasing the polynomial order, (NxN), where (N) is the interior nodes number of the quadrature.

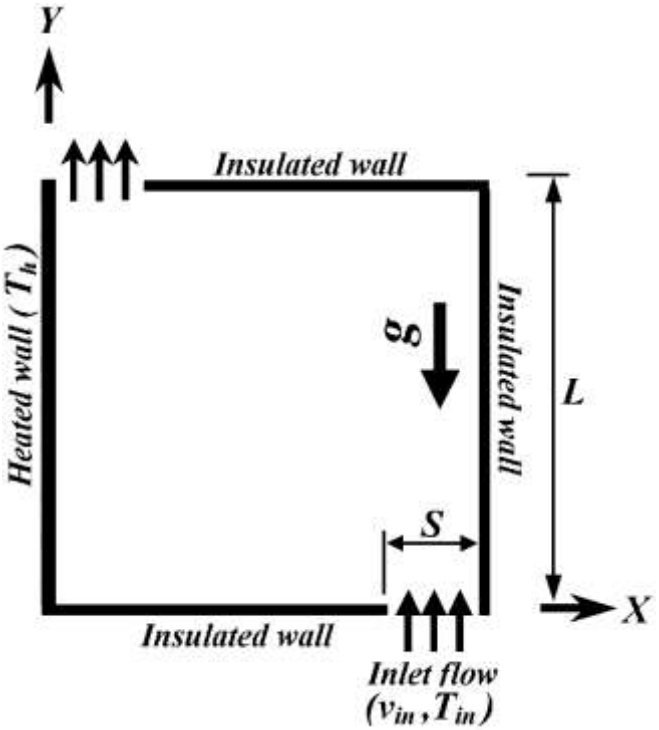

Figure 1. The physical problem.

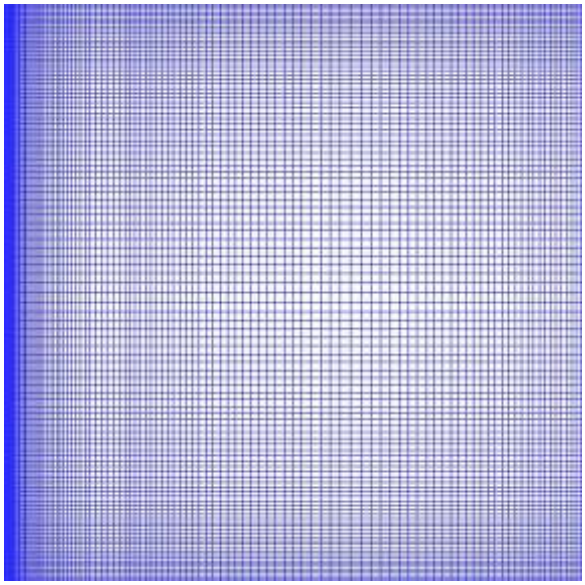

Figure 2. The computational mesh employed.

3. VALIDATION

The numerical model used to simulate the enclosure in this paper was validated using Angirasa research [13]. Angirasa examined in detail The interaction between the buoyancy and the forced. Both positive and negative temperature potentials are considered. Angirasa observed Anomalous heat transfer behavior where the interaction becomes quite complex. At higher absolute values of the Grashof number. Figure (3) shows a comparison between local Nusselt number along the hot wall for Angirasa results and the current results aimed at the case of Opposing flow. Good approximation was found between Angirasa results and the results of the current paper. The discretized energy and vorticity-transport equations are simultaneously solved using the alternating direction implicit scheme (ADI), and the stream function equation is solved with the successive over relaxation method (SOR). The validation took place at the following parameters, Grashof number $=10^6$, Prandtl number =0.7, Richardson number = 10.

Which means Reynolds number = 316.22776.

$$Ri = \frac{Gr}{\mathrm{Re}^2} \tag{6}$$

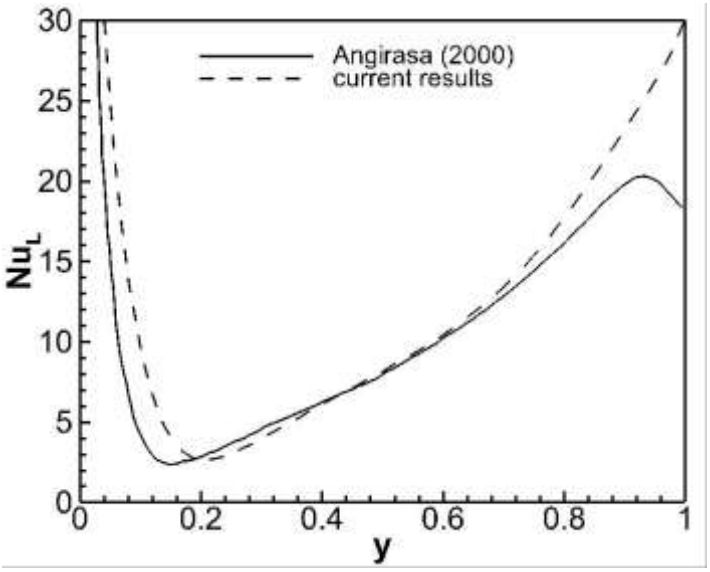

Figure 3. Verification.

4. RESULTS AND DISCUSSION

The objective of the study is to investigate the effect of heating the enclosure at different Reynolds numbers. The relationship between the average Nusselt number and Reynolds number was outlined in figure (4), for Richardson numbers $\left(Gr/\mathrm{Re}^2\right)$ varying from 0 to 5. The values of Reynolds number that were tested ranged between 25 to 300. Figure (4) shows that by enlarging the values of Reynolds number and Richardson numbers, the turbulence in the enclosure cavity increased significantly leading to more heat to be transferred from the fluid near the heated wall to the fluids far neat the insulated walls, consequently the values of average Nusselt number would be enlarged.

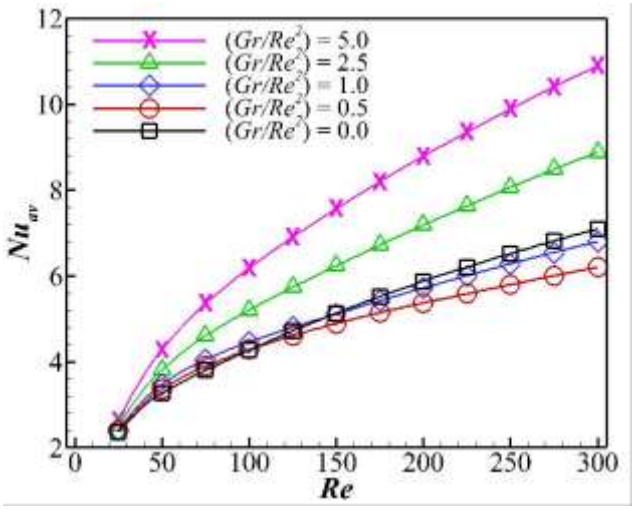

Figure 4. Variation of average Nusselt number with Reynolds number for different Richardson numbers.

Distribution of local Nusselt number through the heated wall are shown in figures (5-9) as the Richardson numbers changed from 0 to 5, for different values of Reynolds number. For 0 Richardson numbers in figure (5), the Nusselt number start with a straight line for all the values of Reynolds number. As the Richardson numbers and Reynolds number increased from figure (7-9) the Nusselt number start with a peak at the lower point of the heated wall and then decreased, followed by an increase. It should be outlined that when the heating is from the side of the cavity, oscillatory behavior is regularly met when the Reynolds number is high enough and through the transition phase from one flow structure to another. Full circles is used to report the unsteady solutions. They are characterized by keeping periodic oscillations through time and throughout flow cycles, they are found as mean values calculated. These periodic existence range solutions hang on strongly on Reynolds number as clearly shown. In general, the local Nusselt in figures (5-9) was as shown in figure (4) increases by increasing the values of Reynolds and Richardson numbers.

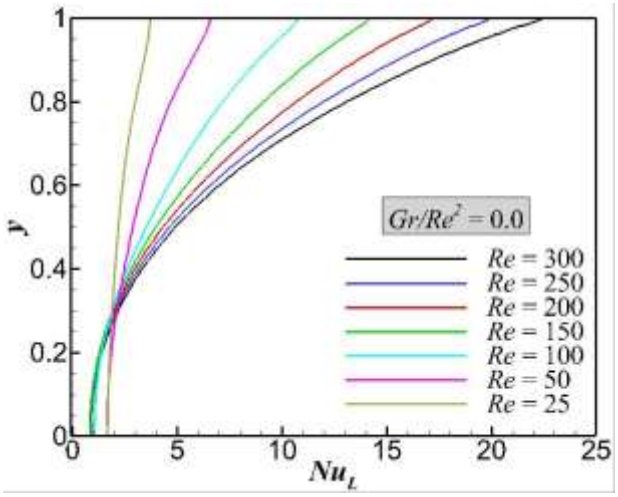

Figure 5. Local Nusselt number distributions along the heated wall at Ri=0 and different Reynolds numbers.

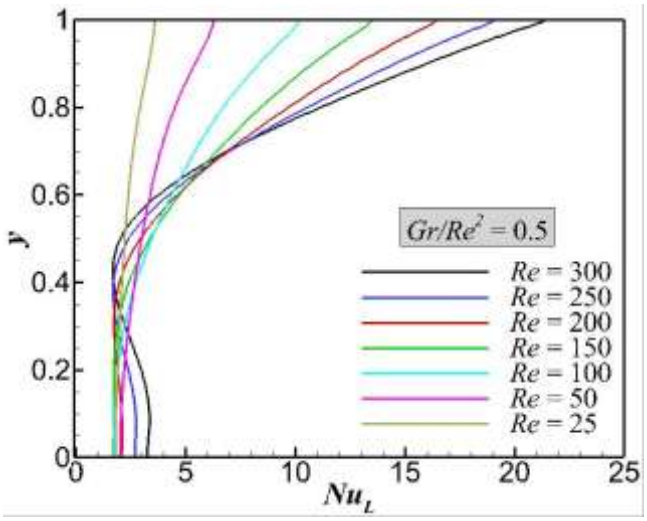

Figure 6. Local Nusselt number distributions along the heated wall at Ri=0.5 and different Reynolds numbers.

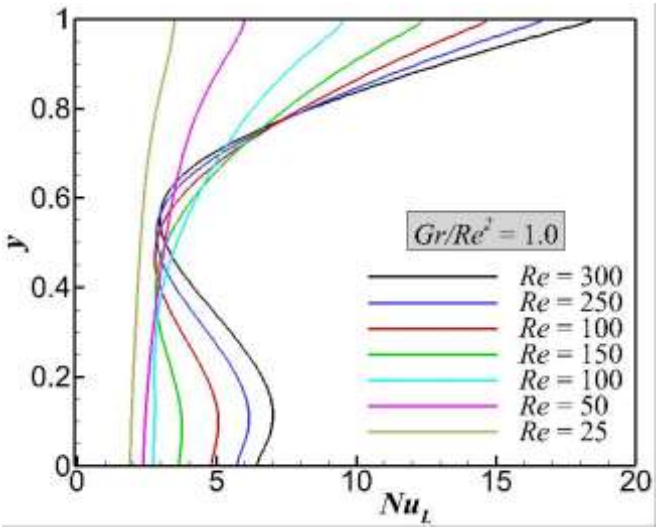

Figure 7. Local Nusselt number distributions along the heated wall at Ri=1.0 and different Reynolds numbers.

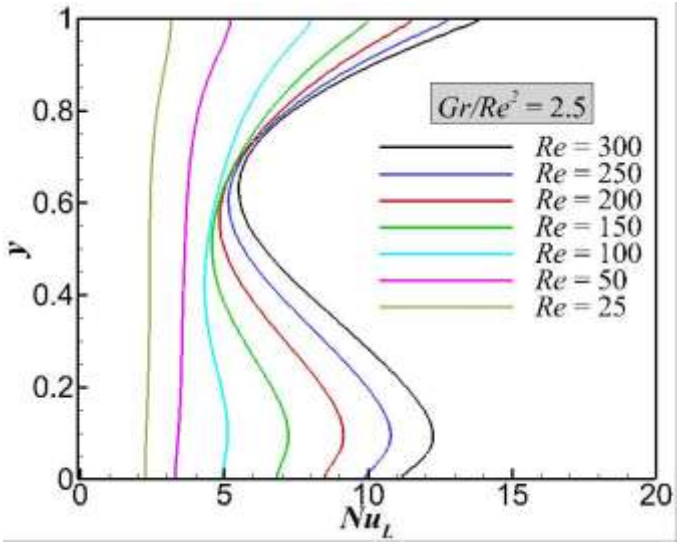

Figure 8. Local Nusselt number distributions along the heated wall at Ri=2.5 and different Reynolds numbers.

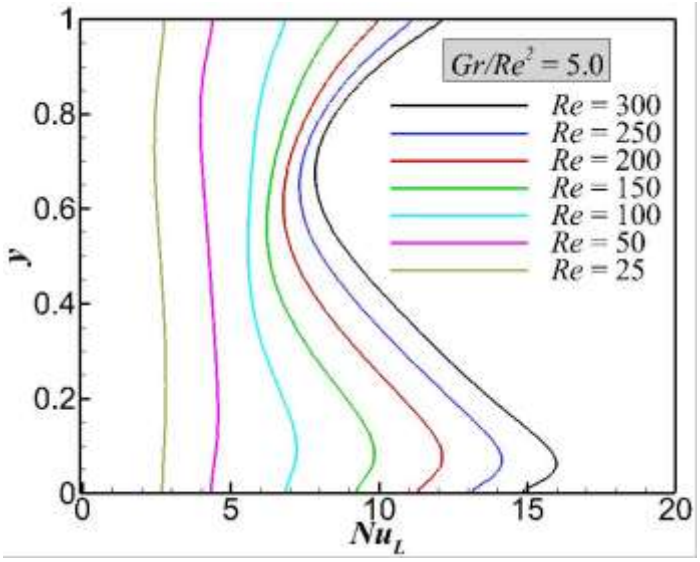

Figure 9. Local Nusselt number distributions along the heated wall at Ri=5.0 and different Reynolds numbers.

Observing the isothermal contours in figure (10-14) it illustrated how the isothermal lines changes from almost being vertical lines at small Reynolds number to being horizontal lines at high Reynolds number. This indicates that the variation of Reynolds number effects the heat transfer mechanism. For small Reynolds number, conduction is dominated on the heat transfer. As the. As Reynolds number increases, the effect of buoyancy increases leads to the isotherms pattern stratification due to the currents of stronger convective currents, meanwhile the conduction is inhibited simultaneously. Consequently, increasing Reynolds number alternate the mode of heat transfer from being dominated by conduction to being dominated by convection. This alternate in the mode of heat transfer in this investigation can be set for Reynolds number between 25 and 300, where the membrane starts to deform and the isotherms start to convert horizontal. Figures (10-14) show the streamlines as well. In figure (10) with 25 Reynolds number and 0 Richardson number, the streamlines of the cavity have two small vortices at an opposite corner, as the Reynolds number increases the vortices enlarged for the same Richardson number. Increasing Reynolds and Richardson numbers in figures (11-14) increased the number of vortices developed in the enclosure, due to the increases in the turbulence and the heat transferred from the heated sidewall.

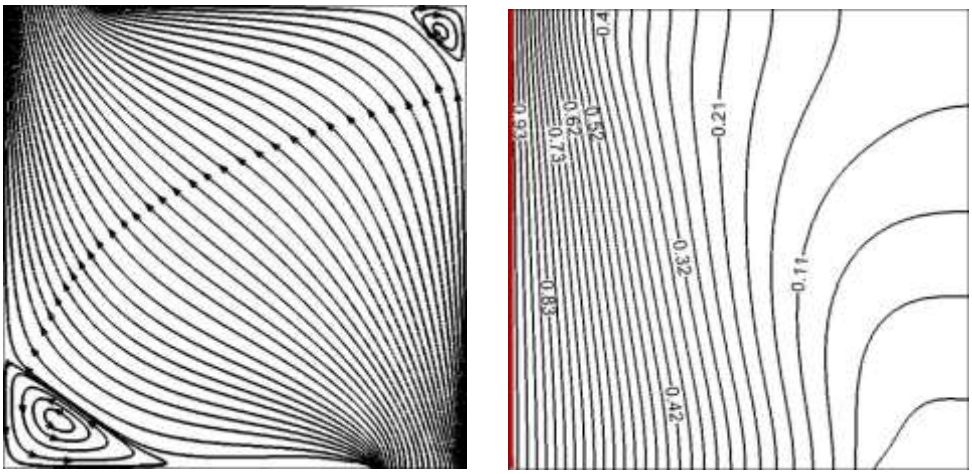

(a) Re = 25

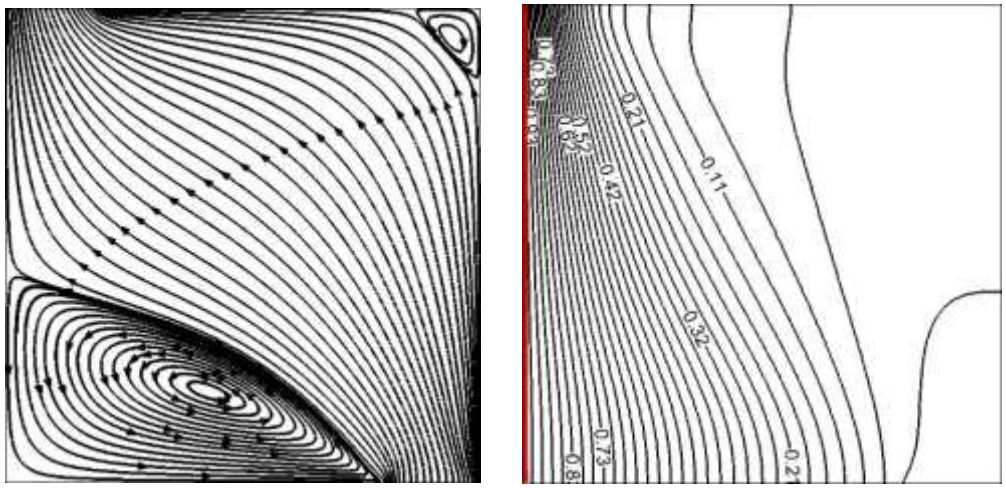

(b) Re = 50

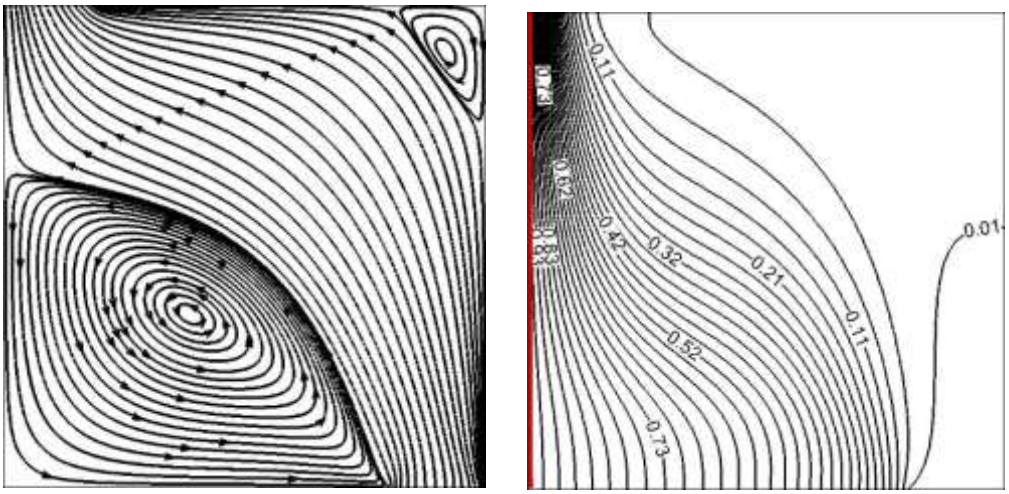

(c) Re = 100

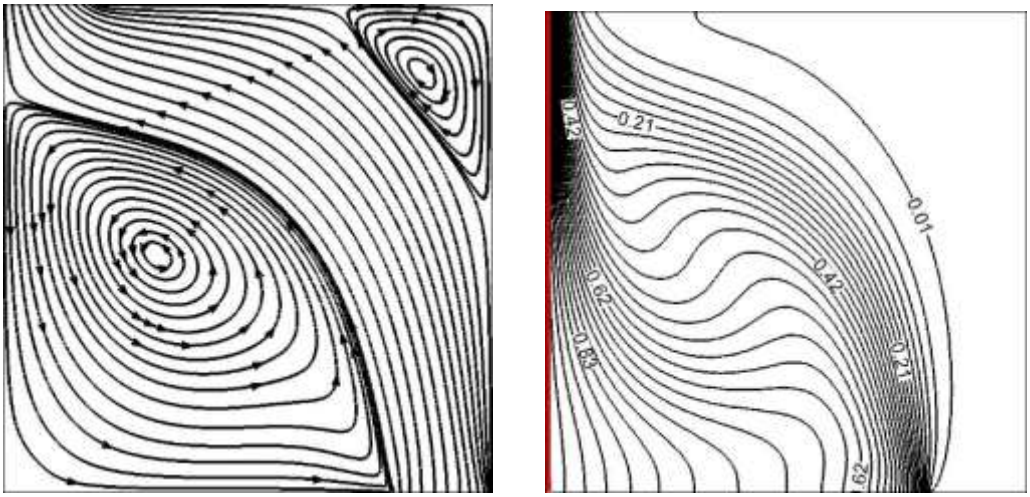

(d) Re = 300

Figure 10. Streamline and isotherm patterns for mixed convective flow at different Reynolds number (a) Re=25, (b) Re=50, (c) Re=100, and (d) Re=300 and at Ri=0.0 (No Heating).

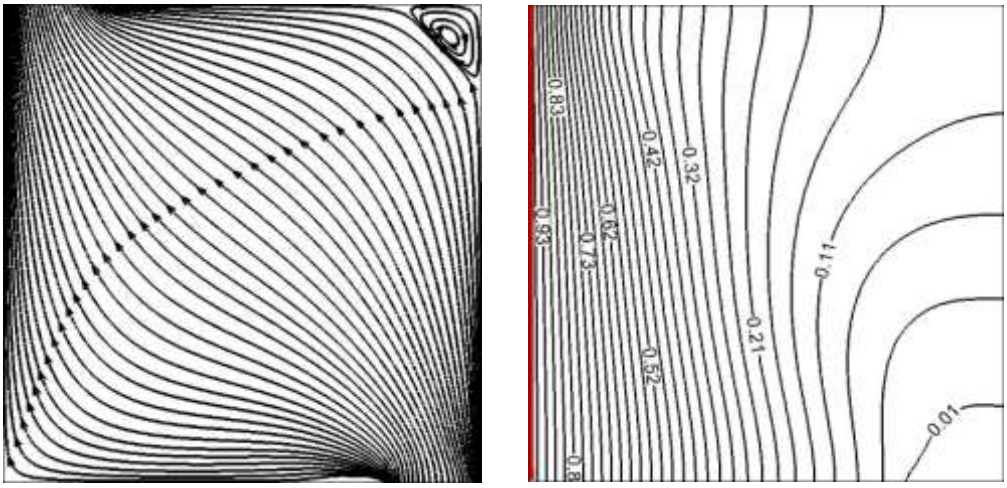

(a) Re = 25

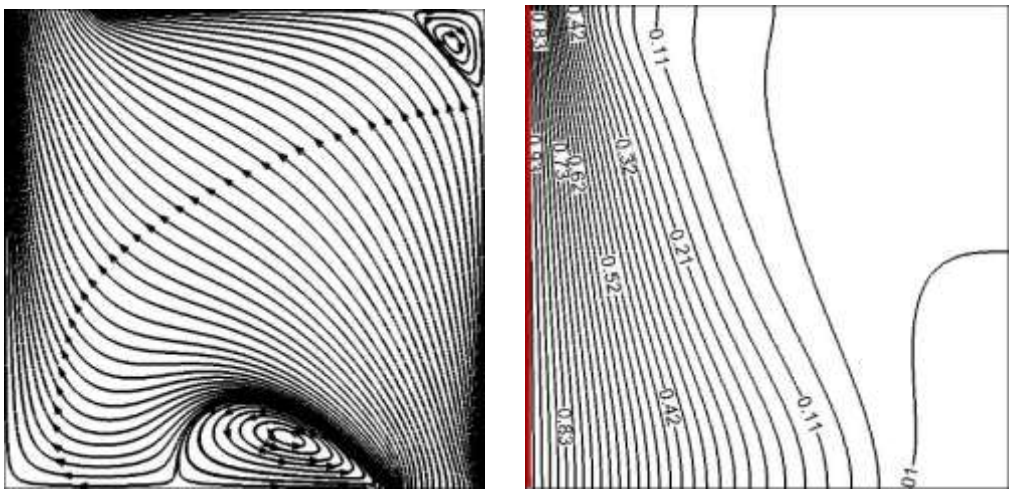

(b) Re = 50

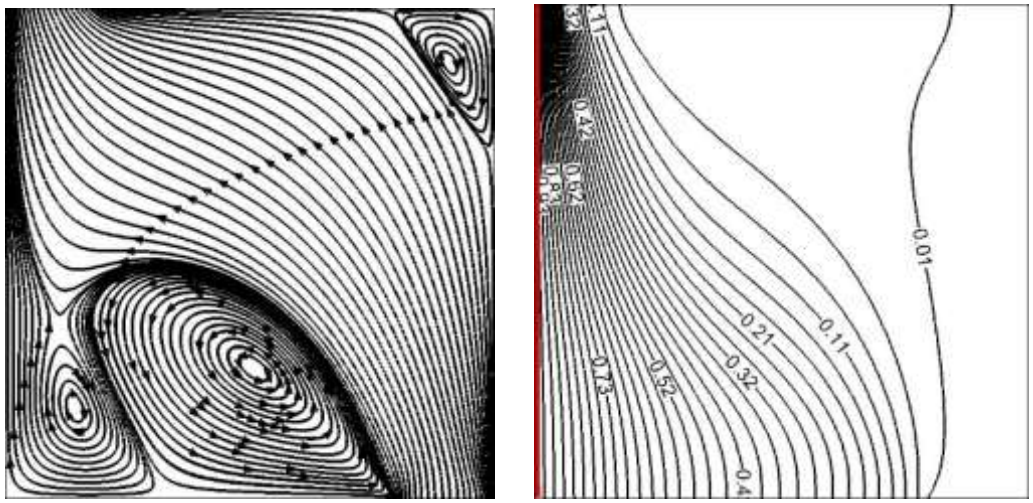

(c) Re = 100

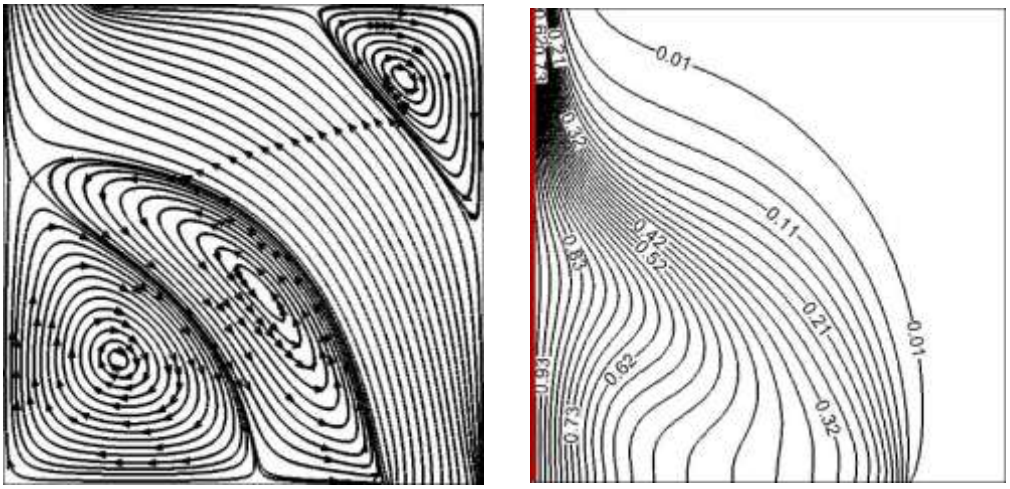

(d) Re = 300

Figure 11. Streamline and isotherm patterns for mixed convective flow at different Reynolds number (a) Re=25, (b) Re=50, (c) Re=100, and (d) Re=300 and at Ri=0.5.

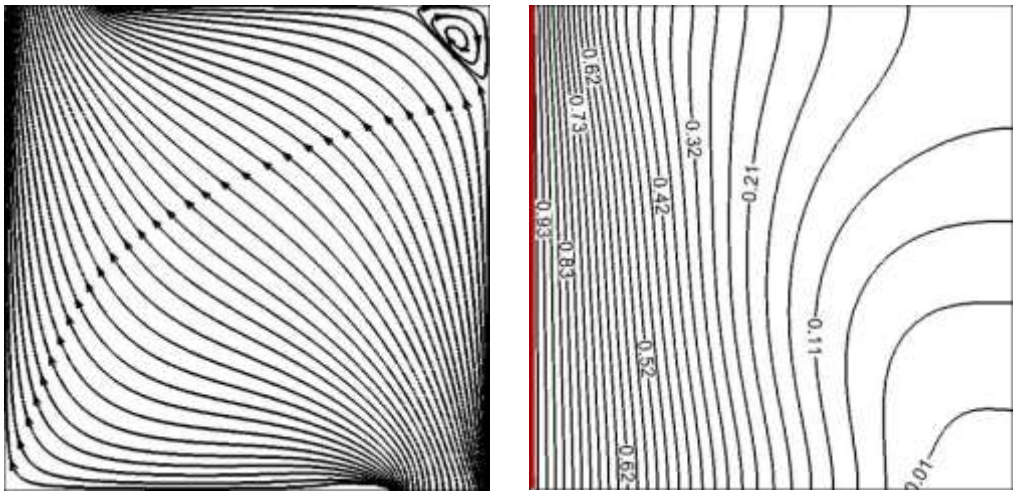

(a) Re = 25

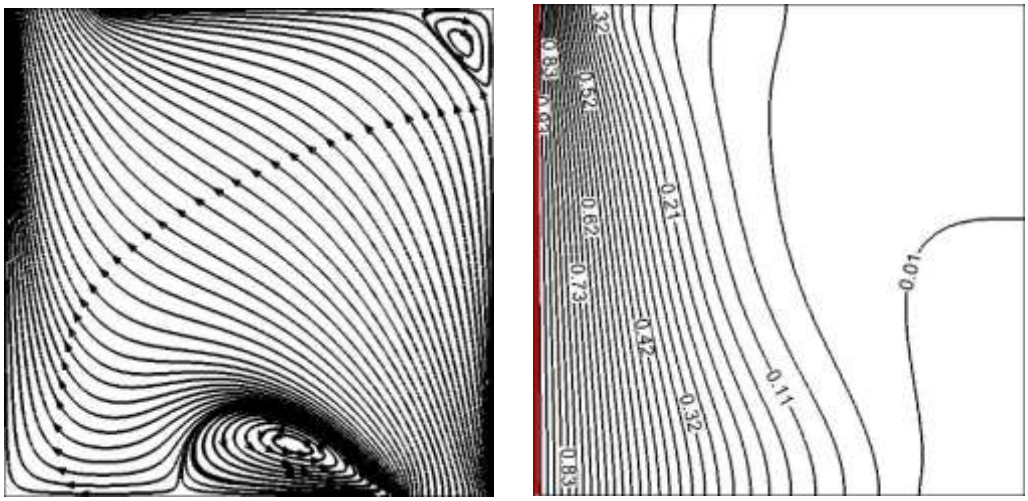

(b) Re = 50

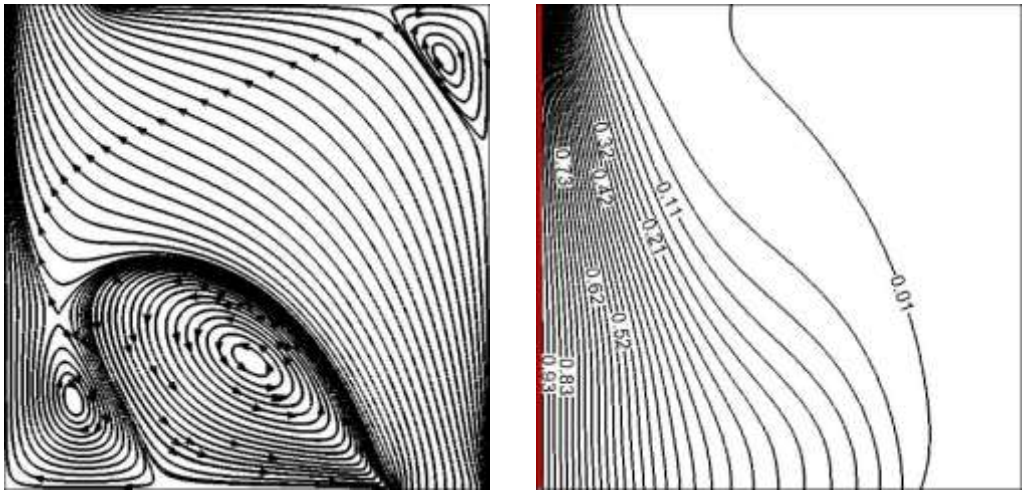

(c) Re = 100

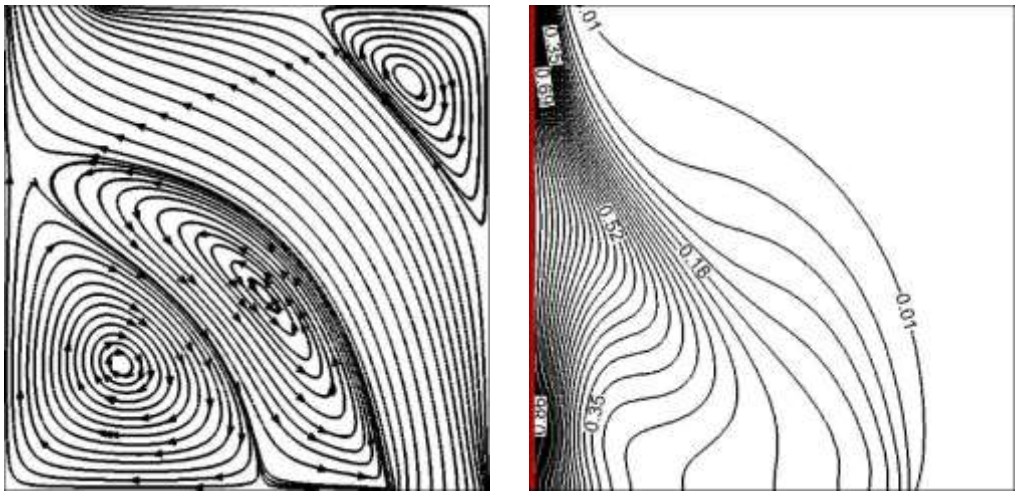

(d) Re = 300

Figure 12. Streamline and isotherm patterns for mixed convective flow at different Reynolds number (a) Re=25, (b) Re=50, (c) Re=100, and (d) Re=300 and at Ri=1.0.

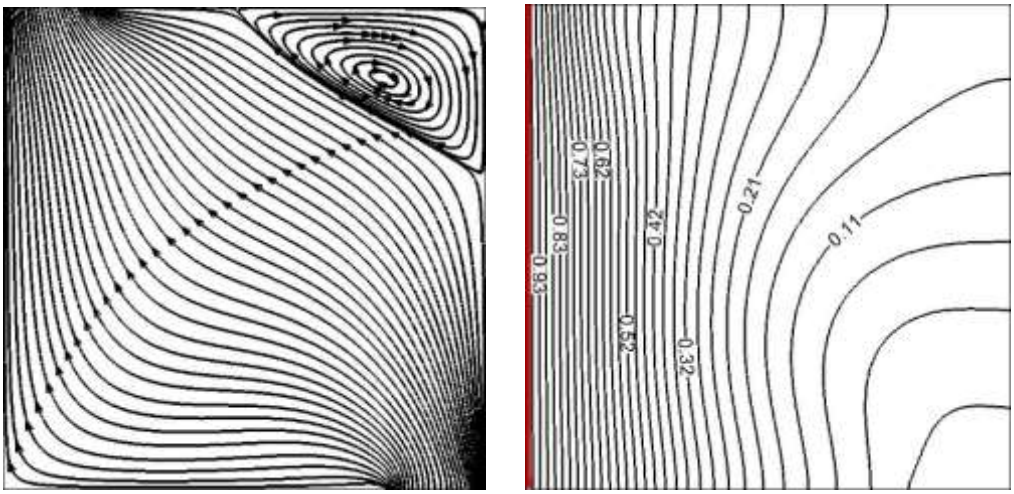

(a) Re = 25

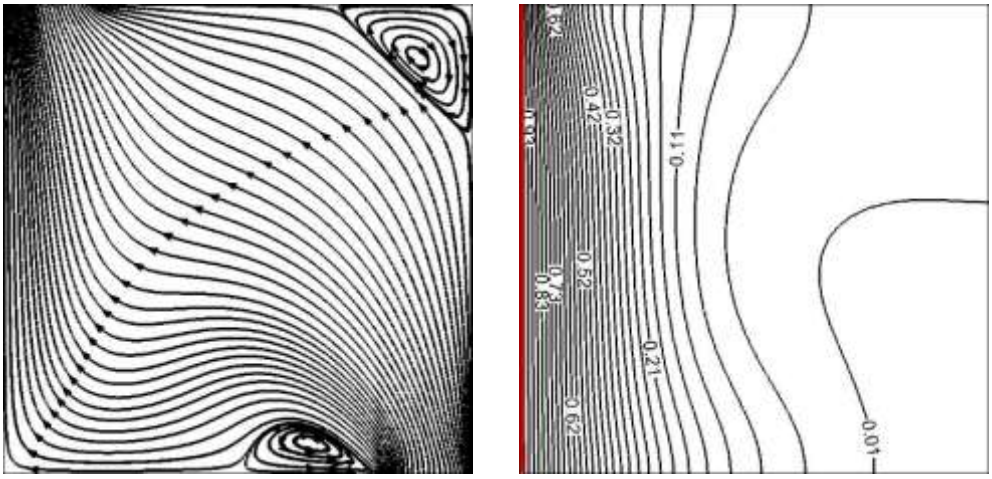

(b) Re = 50

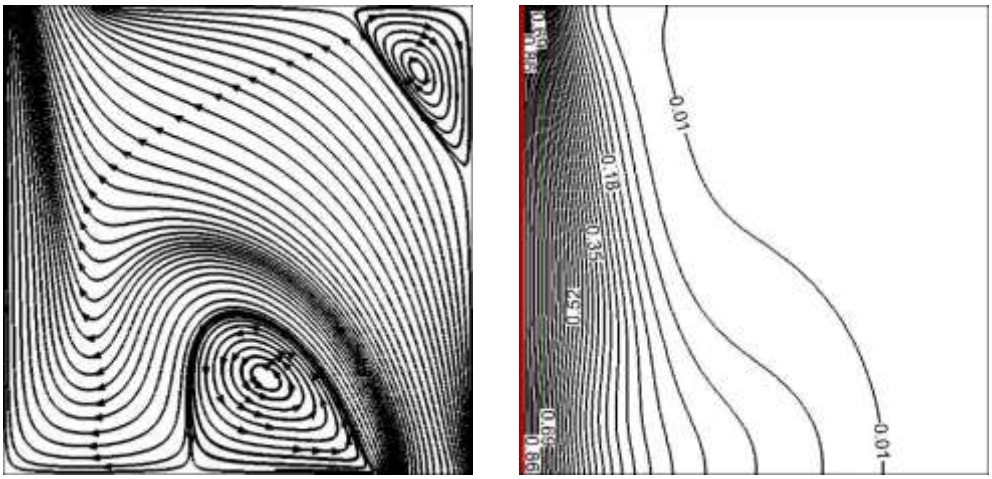

(c) Re = 100

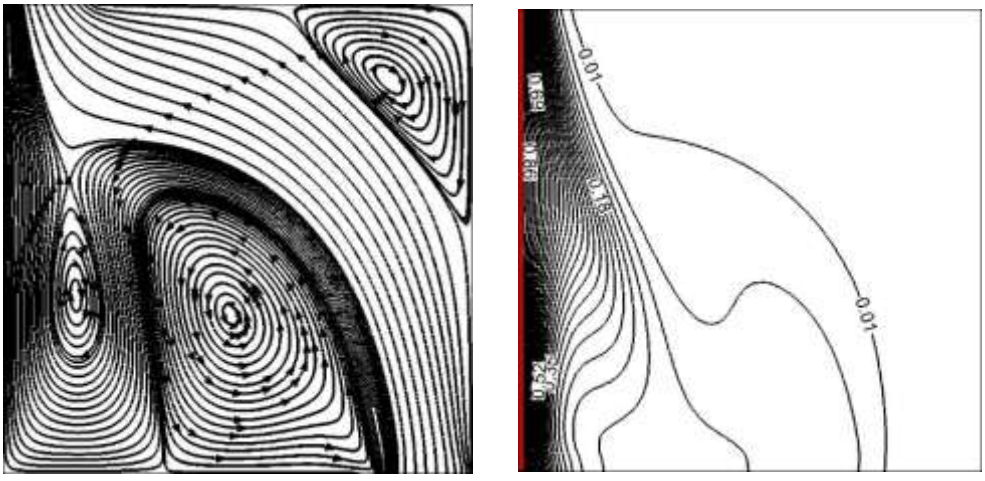

(d) Re = 300

Figure 13. Streamline and isotherm patterns for mixed convective flow at different Reynolds number (a) Re=25, (b) Re=50, (c) Re=100, and (d) Re=300 and at Ri=2.5.

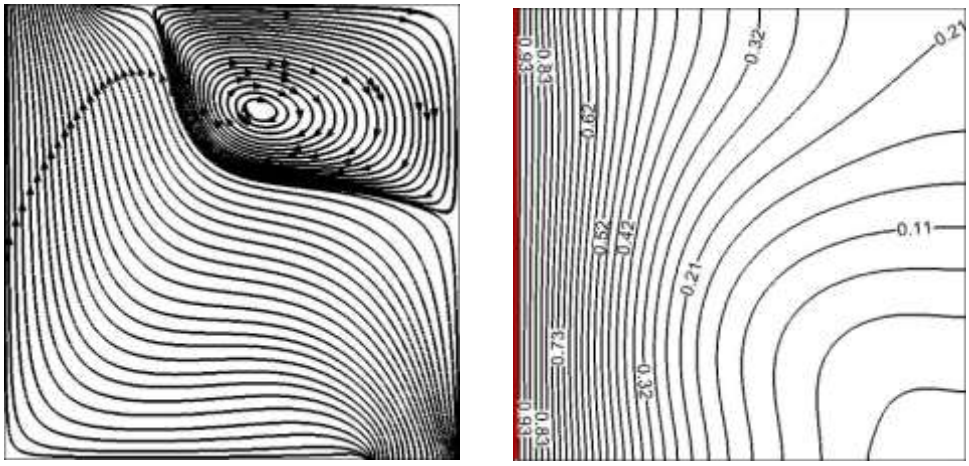

(a) Re = 25

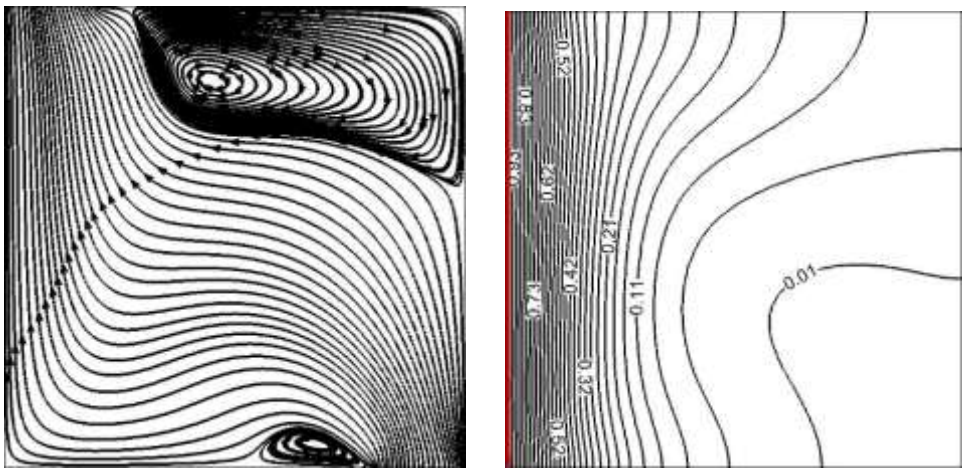

(b) Re = 50

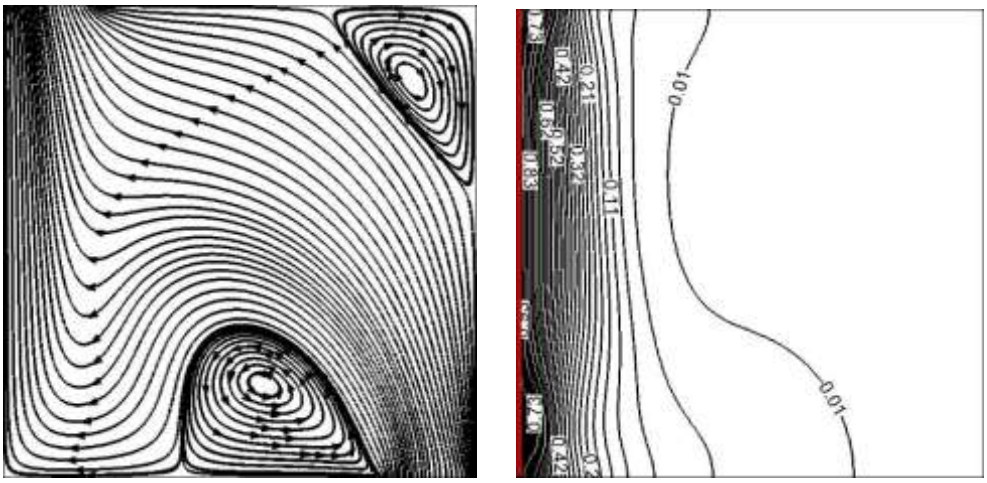

(c) Re = 100

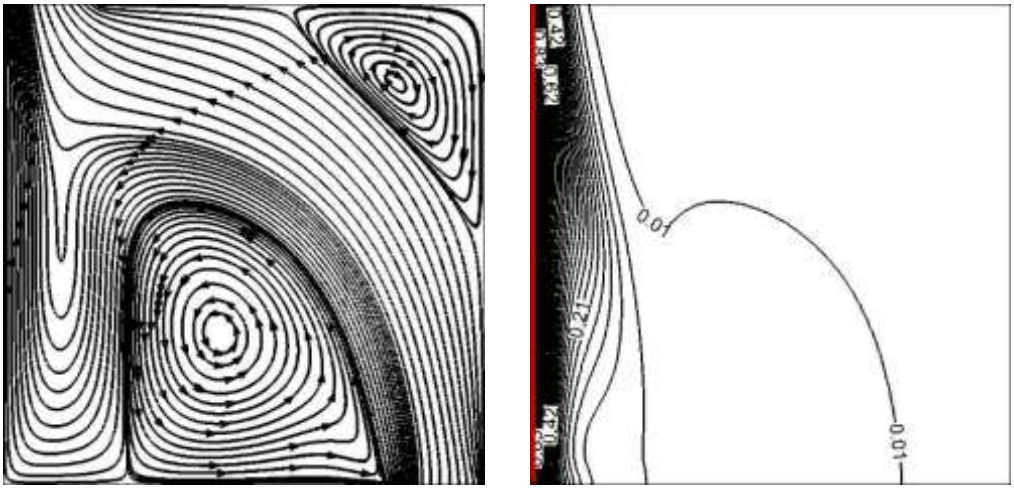

Figure 14. Streamline and isotherm patterns for mixed convective ow at different Reynolds number (a) Re=25, (b) Re=50, (c) Re=100, and (d) Re=300 and at Ri=5.0.

CONCLUSIONS

The paper numerically study the enclose with force and free heat convection. Galerkin finite element approach was used for the numerical analysis, the investigated enclosure are square geometry with an inlet at the bottom and an opposite outlet at the top. Heat was applied to one side of the enclosure while the other walls was set as an insulated wall. It was concluded that:

1- Nusselt number enlarged as the Richardson number increases.

2- Nusselt number enlarged as the Reynolds number increases.

3- Vortices inside the enclosure enlarged as the Richardson number increased.

4- Vortices inside the enclosure enlarged as the Reynolds number increased.

5- Isothermal lines changed from vertical position to horizontal one as the Reynolds number increases.

6- Isothermal lines shifted to the heated wall as the Richardson number increases.

REFERENCES

[1] S. Izadi, T. Armaghani, R. Ghasemiasl, A.J. Chamkha, and M. Molana, "A comprehensive review on mixed convection of nanofluids in various shapes of enclosures", Ptec., 2018, https://doi.org/10.1016/j.powtec.2018.11.006.

[2] D.H. Fontes, D.D.O. Santos, E.L.M. Padilla, and E.P.B. Filho, "Two numerical modelings of free convection heat transfer using Nano fluids inside a square enclosure", Mechanics Research Communications, (2015), http://dx.doi.org/10.1016/j.mechrescom.2015.03.009.

[3] I.V. Miroshnichenko, and M.A. Sheremet, "Turbulent natural convection heat transfer in rectangular enclosures using experimental and numerical approaches: A review", Renewable and Sustainable Energy Reviews, Vol. 82, Pp. 40–59, 2018.

[4] L.M. Al-Balushi, M.J. Uddin, and M.M. Rahman, "Natural convective heat transfer in a square enclosure utilizing magnetic nanoparticles", Propulsion and Power Research, Vol. 8, No. 3, Pp. 194-209, 2019.

[5] S.A.M. Mehryan, M. Ghalambaz, R.K. Feeoj, A. Hajjar, and M. Izadi, "Free convection in a trapezoidal enclosure divided by a flexible partition", International Journal of Heat and Mass Transfer, Vol. 149, Pp. 119-186, 2020.

[6] K. Venkatadri, O. Anwar B´eg , P. Rajarajeswari, and V.R. Prasad, "Numerical simulation of thermal radiation influence on natural convection in a trapezoidal enclosure: heat flow visualization through energy

flux vectors", International Journal of Mechanical Sciences, 2019, doi: https://doi.org/10.1016/j.ijmecsci.2019.105391.

[7] D. Groulx, P.H. Biwole, and M. Bhouri, "Phase change heat transfer in a rectangular enclosure as a function of inclination and fin placement", International Journal of Thermal Sciences, Vol. 151, Pp. 106-260, 2020.

[8] A.C. Bourdillon, P.G. Verdin, and C.P. Thompson, "Numerical simulations of water freezing processes in cavities and cylindrical enclosures", Applied Thermal Engineering, Vol. 75, Pp. 839-855, 2015.

[9] K. Ezzaraa, A. Bahlaoui, I. Arroub, A. Raji, M. Hasnaoui, and M. Naïmi, "Radiation effect on mixed convection cooling in a ventilated horizontal cavity with multiple ports", International Journal of Mechanical Sciences, 153–154, Pp. 310–320, 2019.

[10] S.Y. Motlagh, E. Golab, and A.N. Sadr, "Two-phase modeling of the free convection of nanofluid inside the inclined porous semi-annulus enclosure", International Journal of Mechanical Sciences, Vol. 164, Pp. 105-183, 2019.

[11] J.R. Lee, "Numerical simulation of natural convection in a horizontal enclosure: Part I. On the effect of adiabatic obstacle in middle", International Journal of Heat and Mass Transfer, Vol. 124, Pp. 220–232, 2018.

[12] S.H. Park, Y.M. Seo, M.Y. Ha, and Y.G. Park, "Natural convection in a square enclosure with different positions and inclination angles of an elliptical cylinder Part I: A vertical array of one elliptical cylinder and one circular cylinder", International Journal of Heat and Mass Transfer, Vol. 126, Pp. 173–183, 2018.

[13] C. Qi, J. Tang, Z. Ding, Y. Yan, L. Guo, and Y. Ma, "Effects of rotation angle and metal foam on natural convection of nanofluids in a cavity under an adjustable magnetic field", International Communications in Heat and Mass Transfer, 109, Pp. 104-349, 2019.

[14] P. Zhang, X. Zhang, J. Deng, and L. Song, "A numerical study of natural convection in an inclined square enclosure with an elliptic cylinder using variational multiscale element free Galerkin method", International Journal of Heat and Mass Transfer, 99, Pp. 721–737, 2016.